Reac Kinet Mech Cat (2017) 121:453–472
DOI 10.1007/s11144-017-1168-0

Influence of the Zn–Al binary oxide composition on the physicochemical and catalytic properties of Ni catalysts in the oxy-steam reforming of methanol

Paweł Mierczynski[1] · Magdalena Mosinska[1] · Mateusz Zakrzewski[1] · Bartosz Dawid[1] · Radoslaw Ciesielski[1] · Waldemar Maniukiewicz[1] · Tomasz Maniecki[1]

Received: 30 November 2016 / Accepted: 25 February 2017 / Published online: 10 March 2017

Abstract This paper presents the catalytic properties of mono- and bimetallic nickel supported catalysts in the oxy-steam reforming of methanol. The physicochemical properties of the supported catalysts were studied by various techniques such as TPR, TPD-NH_3, XRD and BET. A significant impact of palladium and the support composition on the activity and selectivity of nickel catalysts in OSRM was demonstrated. The highest activity in the oxy-steam reforming of methanol reaction among all nickel catalysts was shown by the 20% Ni/$ZnO{\cdot}Al_2O_3$ (Zn:Al = 1:1) catalyst. The acidity results correlate well with the reactivity of the investigated catalysts. The most active monometallic system showed the highest total acidity and was the easiest to reduce compared to the rest of the investigated Ni catalysts. The effect of palladium on the reducibility and reactivity of the nickel supported catalyst was proven. The activity results carried out in the OSRM reaction showed that such catalytic material may be potentially applied in fuel cell technology.

Keywords Hydrogen production · Oxy-steam reforming of methanol · $ZnO{\cdot}Al_2O_3$ · binary oxide · Nickel catalysts · Palladium, bimetallic catalysts

Introduction

The use of fossil fuels has a negative impact on the environment, causing the emission of harmful oxides into the atmosphere. The emission of harmful gases into the atmosphere is responsible for the formation of smog and the greenhouse effect [1], which presents a serious risk to the human health. In addition, sources of fossil fuels are non-renewable. Their continued exploitation may lead to the depletion of

✉ Paweł Mierczynski
pawel.mierczynski@p.lodz.pl; mierczyn25@wp.pl

[1] Institute of General and Ecological Chemistry, Lodz University of Technology, Zeromskiego 116, 90-924 Lodz, Poland

their sources. Nowadays, the challenge is to obtain energy from renewable sources. One of the possible alternatives to fossil fuels is hydrogen [2]. It can be a fuel of the future because it is an eco-environmentally friendly source of energy. Hydrogen combustion generates large amounts of heat and the only product of this process is water vapor. It is worth emphasizing that the sources of hydrogen are practically inexhaustible. Therefore, the hydrogen production is one of the most promising technologies to generate energy.

One of the most promising sources of hydrogen is methanol. It is a good raw material for hydrogen production because it is easily decomposed, which leads to the formation of a hydrogen-rich mixture. Despite the high toxicity, corrosivity and destructive impact on the plastics, methanol has many advantages. It is the simplest alcohol, which has only one carbon in the molecule and is characterized by high hydrogen to carbon ratio. All of these properties indicate, that the oxy-steam reforming of methanol process can be potentially applied to hydrogen production at low temperature (180–330 °C), without a carbon deposit formation [3–6]. The OSRM is a combination of two processes, namely steam reforming and partial oxidation of methanol. It is an energetically favorable process because this reaction runs in the auto-thermal way, without the need to supply any external heat [7–10].

The literature review showed that typical catalytic system using in the oxy-steam reforming of methanol reaction are monometallic: Ni [10–13], Cu [5, 14, 15], Co, Fe, Pd [16, 17], Pt, Ru, Ir, Ag, Au and bimetallic: M–CuO/ZnO/Al_2O_3, where M = Pt, Pd, Rh, Ru [18, 19] supported catalysts.

Furthermore, nickel supported catalysts are widely used in many other processes such as oil refining, hydrocracking, hydrogenation or reforming of hydrocarbons. The active phase of these catalysts is typically metallic nickel supported on various oxides such as γ-Al_2O_3, α-Al_2O_3, SiO_2, ZrO_2, ZnO and CeO_2. It is also well known that the Ni/Al_2O_3 system is very active in the steam reforming reaction of various compounds. Additionally, it is well documented in the literature data that nickel supported catalysts have a high efficiency, good structural and thermal stability compared to the noble metal based catalysts [20, 21].

All of the above mentioned suggestions indicate that hydrogen production via the oxy-steam reforming of methanol reaction is a very important topic nowadays. Therefore, the main goal of this work was to evaluate the effect of support composition on the catalytic and physicochemical properties of the nickel supported catalysts in OSRM reaction. Another important aim of the work was to study the impact of palladium on reactivity of nickel catalysts in OSRM process. In order to achieve the intended purposes of the work we prepared mono-Ni and bimetallic Pd–Ni catalysts supported on various binary oxides and tested their reactivity in OSRM reaction.

Experimental

Preparation of the catalytic systems

Supports material

Binary oxide $ZnO{\cdot}Al_2O_3$ (Zn:Al = 2:1, 1:1, 1:2, 1:4) systems were prepared by co-precipitation method. In order to prepare binary oxides with the various molar ratio of Zn:Al = 2:1, 1:1, 1:2, 1:4, the aqueous solutions of zinc nitrate (1 mol/L) and aluminum nitrate (1 mol/L) have been mixed in an appropriate amount with constant stirring at a temperature of 80 °C. Then, in the next step of the synthesis of the supports, a concentrated ammonia solution was added into a mixture until the pH of the solution reached a value between 10 and 11. Thereafter, the solution was stirred for 30 min. In the next step, the resulting precipitate was washed with deionized water. A purified precipitate was firstly dried at 120 °C for 15 h and calcined in air atmosphere for 4 h at 400 °C.

Preparation of monometallic and bimetallic catalysts

Monometallic nickel catalysts supported on various supports $ZnO{\cdot}Al_2O_3$ (Zn:Al = 2:1, 1:1, 1:2, 1:4) were prepared by the wet aqueous impregnation method. A nickel nitrate (V) was used as a precursor of NiO phase. Then the prepared catalysts were dried for 2 h in air atmosphere at 120 °C and finally calcined for 4 h at the same atmosphere at 400 °C. Bimetallic supported catalysts were prepared by a subsequent impregnation method. The palladium phase was introduced on the surface of the monometallic nickel catalyst from palladium nitrate (V) solution. In the next step, the obtained catalysts were dried for 2 h in air at 120 °C, and afterwards they were calcined for 4 h at 400 °C also in air. The nickel content was 20 wt% in all cases, whereas the palladium content in the bimetallic systems was 0.5 and 2 wt%, respectively.

Characterization of the catalytic material

Specific surface area measurements

The specific surface area measurements of supported catalysts were determined by the BET method based on low temperature (77 K) nitrogen adsorption in a Sorptomatic 1900 Carlo-Erba apparatus. The pore size distributions were determined based on BJH method.

Temperature programmed reduction (TPR-H_2)

Temperature programmed reduction measurements were performed in order to study the reducibility of the prepared catalysts. The reduction behavior for all systems was studied in the temperature range of 25–900 °C with a heating rate of

10 °C min^{-1}. Each measurement was carried out using an automated apparatus AMI-1. In each test, about 0.1 g of catalyst was placed in a microreactor and was reduced in a mixture of 5% hydrogen in argon stream (5% H_2–95% Ar) with a volumetric flow rate of 40 cm^3 min^{-1}. A thermal conductivity (TCD) detector was used to monitor of hydrogen consumption.

Temperature programmed desorption of ammonia

The acidity of the catalysts was studied using TPD-NH_3 system. The TPD-NH_3 measurements were performed in the temperature range 100–600 °C with a linear heating rate of 25 °C min^{-1}. The measurements for each catalytic material were carried out after removal of physically adsorbed ammonia.

XRD

X-ray diffraction patterns were collected using a PANalytical X'Pert Pro MPD diffractometer. Cu K_α radiation ($\lambda = 154.05$ pm) was used in each measurements. Data were recorded in 2θ angle range of 10°–90°.

Catalytic evaluation of the prepared catalytic systems

The activity of the catalysts were tested in the oxy-steam reforming of methanol (OSRM) using a flow quartz reactor under atmospheric pressure. The OSRM process was carried out at two temperatures 250 and 300 °C. In each test, about 0.2 g of catalyst was placed in the reactor. Then the catalytic system was reduced in a mixture of 5% H_2–95% Ar at 300 °C for 1 h. The composition of the reaction mixture in each test was as follows: $H_2O/CH_3OH/O_2 = 1/1/0.4$ (molar ratio) and the GHSV was 26,700 h^{-1} (calculated at ambient temperature and under atmospheric pressure). The total flow of the reaction mixture was 31.5 ml/min (6% of CH_3OH). Argon gas was used as a balance gas. Catalytic activity tests were carried out after stabilizing the system, in the reaction mixture for 2 h. The analysis of the products formed during the reaction was carried out using GC systems (A precise description of chromatographic analysis was presented in our previous work [8]).

The selectivity to hydrogen, carbon monoxide, carbon dioxide and DME in OSRM was calculated using Eqs. 1–4. The methanol conversion results were calculated based on Eq. 5.

$$S_{H_2}(\%) = \frac{(nH_{2-out})}{\sum \text{products of the reaction}} \times 100 \quad (1)$$

$$S_{CO}(\%) = \frac{(nCO_{out})}{\sum \text{products of the reaction}} \times 100 \quad (2)$$

$$S_{CO_2}(\%) = \frac{(nCO_{2-out})}{\sum \text{products of the reaction}} \times 100 \quad (3)$$

$$S_{DME}(\%) = \frac{(nDME_{out})}{\sum \text{products of the reaction}} \times 100 \quad (4)$$

$$Conv._{CH_3OH} = \frac{n_1^{in}\ CH_3OH - n_2^{out}\ CH_3OH}{n_1^{in}\ CH_3OH} \times 100 \quad (5)$$

Here, $nH_{2\text{-out}}$ is the mole of H_2 in the feed out, $nCO_{2\text{-out}}$ is the mole of CO_2 in the feed out, nCO_{out} is the mole of CO in the feed out, $nDME_{out}$ is the mole of DME in the feed out, n_1^{in} CH_3OH, n_2^{out} CH_3OH is the mole of CH_3OH in the feed in and in the feed out.

Results and discussion

The specific surface area of the catalytic materials

The specified values of the catalyst surface area (SSA), monolayer capacity and average pore radius for monometallic nickel supported catalysts are given in Table 1 and Fig. 1. The specific surface area measurements performed for monometallic nickel catalysts showed that the SSA value increases in parallel with the increase of aluminum content in the catalytic system. The highest value of SSA equal to 246 m^2/g was found for the nickel catalyst supported on binary oxide with the highest content of Al. Similar behavior was observed in the case of the monolayer capacity value. In contrast, zinc oxide had the lowest surface area (3.4 m^2/g) compared to the rest catalytic systems. The specific surface area measurements showed that catalyst (20% $Ni/ZnO{\cdot}Al_2O_3$, in which Zn:Al = 2:1) containing the largest amount of zinc had the lowest value of SSA compared to the others Ni supported catalysts. The specific surface area measurements performed for bimetallic supported catalysts showed that addition of a small amount of palladium (0.5 or 2 wt%) into 20% $Ni/ZnO{\cdot}Al_2O_3$ catalyst (Zn:Al = 1:1) causes a slight

Table 1 BET surface area, monolayer capacity and average pore radius of mono- and bimetallic nickel catalysts supported on binary oxide calcined in air atmosphere at 400 °C for 4 h

Material	BET surface area (m^2/g)	Monolayer capacity (cm^3/g)	Average pore radius (nm)
20% $Ni/ZnO{\cdot}Al_2O_3$ (Zn:Al = 2:1)	108	24.7	2.5
20% $Ni/ZnO{\cdot}Al_2O_3$ (Zn:Al = 1:1)	123	28.3	1.9
20% $Ni/ZnO{\cdot}Al_2O_3$ (Zn:Al = 1:2)	231	53.2	1.9
20% $Ni/ZnO{\cdot}Al_2O_3$ (Zn:Al = 1:4)	246	56.4	1.9
0.5% Pd–20% Ni/(Zn:Al = 1:1)	106	24.4	2.6
2% Pd–20% Ni/(Zn:Al = 1:1)	104	23.9	2.6

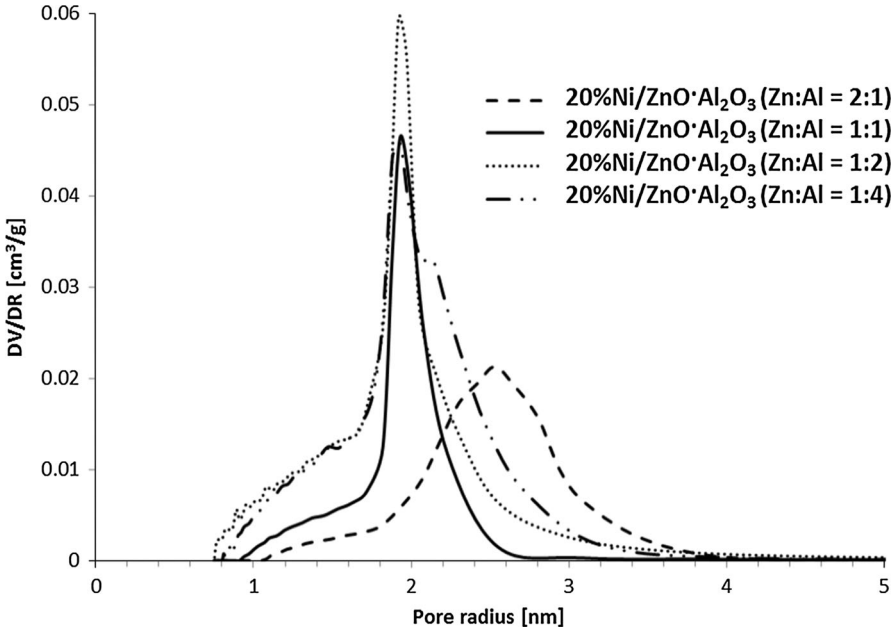

Fig. 1 Pore radius distributions for monometallic nickel supported catalysts calcined at 400 °C in air atmosphere for 4 h

decrease of the SSA value. The results of specific surface area performed for bimetallic supported catalysts showed that both catalytic systems had practically the same values of SSA. On the other hand, specific surface area measurements carried out for all catalysts showed that the value of the average pore radius are practically the same for all monometallic nickel systems (see Fig. 1.). Concerning the average pore size, the results indicate that all nickel supported catalysts have an average pore size of about 1.9 nm. Only nickel catalyst with the highest content of zinc showed the average pore size about 2.5 nm. The introduction of palladium into nickel supported catalyst resulted in a slight increase in the average pore size obtained for the bimetallic catalysts. The obtained results showed that the average pore size of bimetallic catalysts was about 2.6 nm (see Fig. 2).

Influence of the Al content and palladium on the reducibility of Ni catalysts

The catalysts reducibility was determined using temperature programmed reduction (TPR-H_2). In order to explain the interaction between NiO and support components, the reduction studies for monometallic nickel catalysts supported on Al_2O_3 or ZnO were carried out. The reduction profiles recorded for monometallic nickel catalysts supported on monoxide are shown in Fig. 3. The hydrogen consumption profile recorded for the 20%Ni/ZnO catalyst showed three partially resolved reduction peaks. The first reduction effect with the maximum of hydrogen consumption rate at about 420 °C, was assigned to the free NiO species reduction. The next peak with

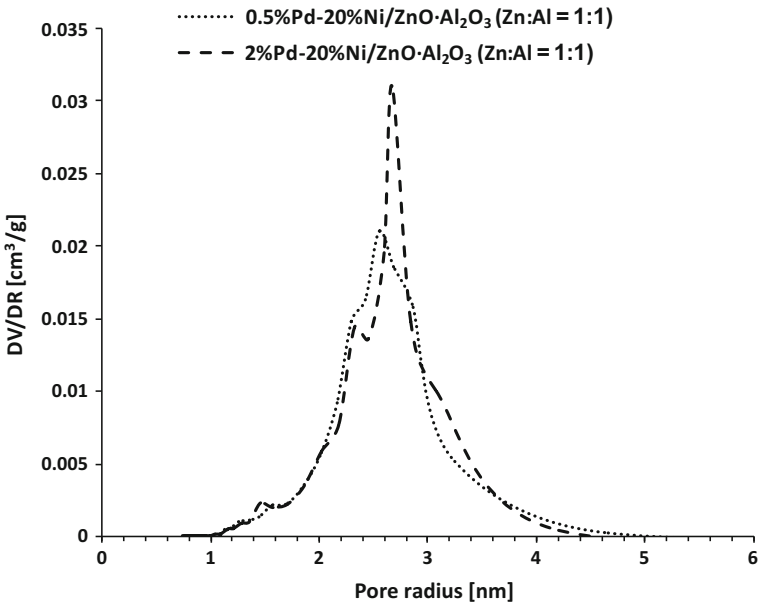

Fig. 2 Pore radius distributions for bimetallic palladium–nickel Pd–Ni/ZnO·Al_2O_3 (Zn:Al = 1:1) supported catalysts calcined at 400 °C in air atmosphere for 4 h

the maximum at about 480 °C is attributed to the reduction of NiO interacted with the support. The last reduction stage located in the temperature range 560–820 °C is connected with the reduction of NiO strongly interacted with support surface. The

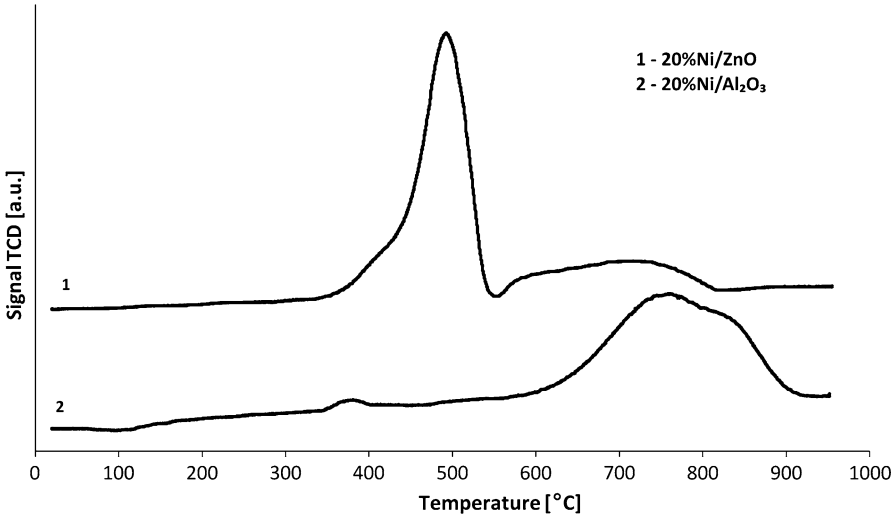

Fig. 3 TPR profiles of monometallic 20% Ni/ZnO and 20% Ni/Al_2O_3 catalysts calcined in air atmosphere for 4 h at 400 °C

reduction study performed for the 20%Ni/Al_2O_3 catalyst showed that this system is reduced in three stages. The first peak located in the temperature range 350–460 °C is assigned to the reduction of free NiO species. The second effect with the maximum of hydrogen consumption at about 740 °C is assigned to the reduction of NiO species strongly interacted with support. The last reduction peak with the maximum of about 800 °C is attributed to the reduction of $NiAl_2O_4$ spinel structure. In conclusion, the reduction study carried out for nickel catalyst supported on aluminum oxide it can be concluded, that most of the NiO is in the strong interactions with the carrier. The proof of this statement is the presence of the two unresolved reduction peaks located at high temperature range. In addition, the high temperature reduction stage situated above 800 °C confirmed the formation of $NiAl_2O_4$ structure during preparation step of the 20%Ni/Al_2O_3 catalyst.

In the next part of the reduction studies, we performed the H_2-TPR measurements for monometallic and bimetallic catalysts supported on various binary oxides. The TPR profiles recorded for monometallic nickel and bimetallic 0.5%Pd–20%Ni/ZnO·Al_2O_3 (Zn:Al = 1:1) or 2%Pd–20%Ni/ZnO·Al_2O_3 (Zn:Al = 1:1) catalysts are shown in Figs. 4 and 5, respectively.

The TPR-H_2 profiles recorded for nickel catalysts supported on binary oxide supports containing the highest content of zinc (Zn:Al = 2:1 or 1:1) showed three reduction stages. The first two reduction effects are connected with the reduction of two kinds of NiO species reduction. The first reduction effects visible on the TPR profiles for both catalysts in the temperature range 150–300 °C are assigned to the unbounded NiO species reduction, while the second TPR peaks, which are connected with the reduction of NiO species strongly interacted with support

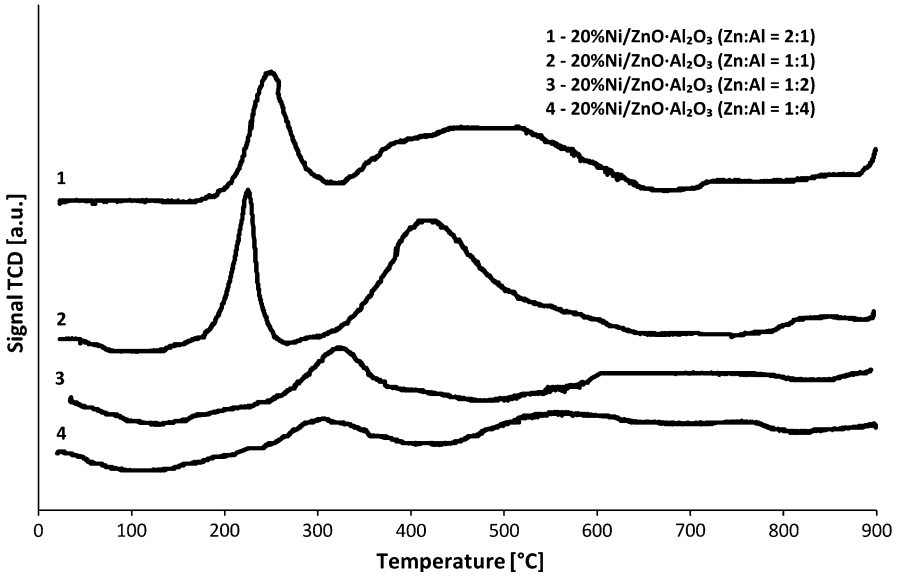

Fig. 4 TPR profiles of monometallic 20% Ni/ZnO·Al_2O_3 catalysts containing various Zn:Al ratio calcined in air atmosphere for 4 h at 400 °C

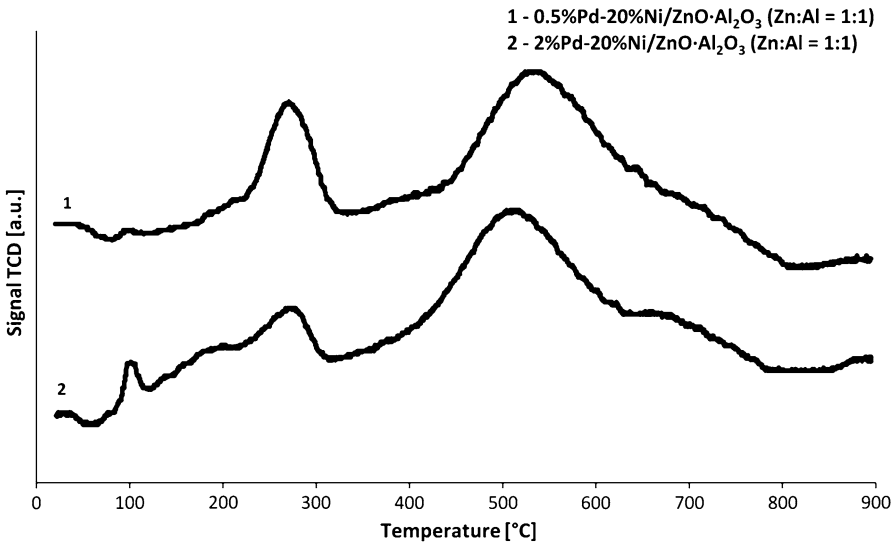

Fig. 5 TPR profiles of bimetallic 0.5%Pd–20%Ni/ZnO·Al_2O_3 (Zn:Al = 1:1) and 2%Pd–20%Ni/ZnO·Al_2O_3 (Zn:Al = 1:1) catalysts calcined in air atmosphere for 4 h at 400 °C

surface were located in the temperature range 300–600 °C. The last high temperature reduction stages visible for both systems on the TPR profiles above 700 °C are assigned to the reduction of the spinel structure $NiAl_2O_4$. Analogous TPR measurements were done for monometallic nickel catalysts supported on binary oxide with higher content of aluminum (Zn:Al = 1:2 or 1:4) and the results are given in Fig. 4. TPR profiles recorded for those catalysts showed the same reduction stages that were observed for the previous investigated nickel supported catalysts. The only difference which was observed on their TPR profiles was a shift of the visible hydrogen consumption peaks towards higher temperature range, as well as the change of their interrelation. In the case of those systems, we observed lower intensity of the hydrogen consumption peaks compared to the systems containing higher content of zinc. The high temperature hydrogen consumption peaks attributed to the spinel structure reduction observed for nickel catalysts with higher contents of aluminum showed higher intensity compared to the systems with lower content of Al. Furthermore, it is worth noting that these systems showed the lower intensity of the reduction stages recorded on the TPR profiles. These results suggest that in these systems, a spinel structure $NiAl_2O_4$ is formed, which is not completely reduced up to temperature of 900 °C.

Kobayashi et al. [22] studied the reducibility of Ni/γ-Al_2O_3 containing different amounts of the nickel oxide phase. They reported that for the catalytic systems with the low nickel content they observed high temperature effect connected with the reduction of nickel aluminate phase. The increase of the Ni content caused the shifts of the observed TPR effect towards lower temperature range, which indicates some interaction between NiO and γ-Al_2O_3. Pairojpiriyakul et al. [20] investigated the

reducibility of 10%Ni/γ-Al_2O_3 and 10%Ni/α-Al_2O_3 catalysts by the temperature programmed reduction technique. The H_2-TPR profile recorded for 10% Ni/γ-Al_2O_3 showed two unresolved reduction stages located in the temperature range 300–650 °C with a maximum consumption of hydrogen at 400 and 600 °C. The TPR profile recorded for 10% Ni/α-Al_2O_3 showed reduction peaks visible in the temperature range 300–550 °C with the maximum of the observed effects situated at about 400 and 520 °C. The peaks observed on the TPR profile at low temperature range 300–450 °C are associated with a reduction of a pure crystalline NiO phase [23]. In the case of the Ni/γ-Al_2O_3 catalyst, the authors observed the high temperature effect at about 550 °C assigned to the $NiAl_2O_4$ spinel structure reduction [24]. These results agree well with our measurements. $NiAl_2O_4$ structure is formed during synthesis of the catalytic systems. The reduction property of Ni catalysts were also studied by Ding et al. [25]. The authors also observed a high temperature effect on the TPR profiles of Ni catalysts attributed to the reduction of spinel $NiAl_2O_4$ structure. Richardson et al. [26]. have reported that during the heat treatment and the impregnation step of the support may take place incorporation of Al^{3+} to the structure of NiO or mutual migration of ions leading to the formation of $NiAl_2O_4$ spinel structure.

Nieva et al. [27] investigated the reducibility of Ni/α-Al_2O_3 and Ni/$ZnAl_2O_4$ catalysts, respectively. They observed one reduction stage in the case of Ni/α-Al_2O_3 catalyst. This reduction stage is connected with the reduction of unbonded NiO species with the maximum of hydrogen consumption peak visible around 390–400 °C. In the case of the nickel catalyst supported on spinel structure, the authors observed a large reduction effect in the temperature range 400–700 °C with a maximum consumption of hydrogen peak around 575 °C. The position of this reduction stage confirmed strong interaction of Ni^{2+} with the spinel $ZnAl_2O_4$ structure.

The reduction studies of bimetallic catalysts were also carried out in this work. TPR profiles of bimetallic 0.5% Pd–20% Ni/ZnO·Al_2O_3 (Zn:Al = 1:1) and 2% Pd–20% Ni/ZnO·Al_2O_3 (Zn:Al = 1:1) catalysts exhibit similar reduction behavior to those found for the above monometallic nickel supported catalysts. At the low temperature range, we observed for both bimetallic catalysts reduction peaks situated at about 100 °C, which were assigned to the reduction of Pd^{2+} to Pd^0. It is also worth emphasizing that bimetallic systems showed the first reduction effects connected with the reduction of unbonded NiO at lower temperature compared to the monometallic catalysts. This shift indicates that the addition of Pd into the nickel catalyst facilitates the reduction of NiO species, because of spillover phenomenon [3, 9, 19, 28–31]. The reduction peaks located at higher temperature were also observed for both systems and are assigned to the reduction of NiO interacted with support. The last reduction stages observed for bimetallic catalysts above 600 °C are assigned to the reduction of $NiAl_2O_4$ spinel structure (see Fig. 5).

Xu et al. [32] studied the reduction behavior of Pd/ZnO/Al_2O_3 catalyst. The TPR profiles recorded for this catalyst also showed a reduction peak in the temperature range 25–100 °C, which is attributed to the reduction of $Pd^{2+} \rightarrow Pd^0$. The reduction behavior of Pd–Ni/Al_2O_3 catalysts was studied in the work [33] and it was shown that addition of palladium into nickel catalyst facilitates its reduction. The

reducibility of the bimetallic Pd–Ni catalysts supported on aluminum oxide was also studied by Lakhapatri et al. [34]. The authors reported that introduction of palladium into nickel supported catalyst decreases the formation of spinel $NiAl_2O_4$ structure and improves the stability of the catalyst as confirmed by our results.

The effect of Zn on the acidity of the nickel supported catalysts

The temperature programmed desorption of ammonia was used to define the acidity and the distribution of acidic centers on the catalyst surface [35, 36]. The distribution of acid centers on the catalyst surface was calculated based on the surface under the peaks at an appropriate temperature range and the obtaining results are given in Table 2. TPD-NH_3 measurements were carried out to determine the influence of the Zn content in the investigated catalysts on the surface acidity. The acidity measurements were conducted over mono and bimetallic catalysts in order to correlate the results of the acidity with their reactivity in OSRM process. It is well known in the literature data [24] that the acidic centers of the catalyst stabilize the intermediates created during the reaction. The TPD-NH_3 results have confirmed that three kinds of acid centers, namely: weak acid, medium-strong and strong acid sites were detected for all investigated catalysts. The results of acidity of the monometallic catalysts calcined at 400 °C in air atmosphere for 4 h shows that 20% Ni/ZnO·Al_2O_3 (Zn:Al = 1:1) and 20% Ni/ZnO·Al_2O_3 systems (Zn:Al = 1:2) had the highest acidity. The lowest value of the total acidity showed nickel catalyst with the highest content of Al. The results of acidity showed that the systems with an average content of Al had the highest value of total acidity. It is worth

Table 2 The amount of NH_3 adsorbed on mono- and bimetallic nickel catalysts calcined in air atmosphere at 400 °C for 4 h

Catalysts		Total acidity (mmol/g) 180–600 °C	Weak centers (mmol/g) 180–300 °C	Medium centers (mmol/g) 300–450 °C	Strong centers (mmol/g) 450–600 °C
Monometallic	20% Ni/ZnO·Al_2O_3 (Zn:Al = 2:1)	0.79	0.2	0.29	0.3
	20% Ni/ZnO·Al_2O_3 (Zn:Al = 1:1)	1.03	0.17	0.38	0.48
	20% Ni/ZnO·Al_2O_3 (Zn:Al = 1:2)	1.02	0.19	0.37	0.46
	20% Ni/ZnO·Al_2O_3 (Zn:Al = 1:4)	0.27	0.09	0.16	0.02
Bimetallic	0.5% Pd–20% Ni/ ZnO·Al_2O_3 (Zn:Al = 1:1)	0.17	0.002	0.05	0.12
	2% Pd–20% Ni/ ZnO·Al_2O_3 (Zn:Al = 1:1)	0.34	0.05	0.05	0.24

emphasizing that the catalyst which exhibited the highest total acidity and had the largest amount of strong acid sites on the catalyst surface was the most active catalyst at 300 °C in OSRM reaction. On the other hand, the system which had the lowest amount of weak acid sites exhibited the highest activity at low temperature of the reaction (250 °C). In the case of the bimetallic Pd–Ni catalysts the results of the acidity showed that the addition of the noble metal into nickel catalyst caused decrease of their total acidity compared to the $Ni/ZnO{\cdot}Al_2O_3$ (Zn:Al = 1:1) supported catalyst. The acidity measurements performed for all catalysts showed that the results of the acidity correlate well with the composition of the obtained catalysts. The catalysts which contain the highest content of the spinel structure phases such as $ZnAl_2O_4$ or $NiAl_2O_4$ exhibited the highest acidity (see next paragraph).

This statement explains the highest total acidity and the highest number of the strong acid sites for $Ni/ZnO{\cdot}Al_2O_3$ (Zn:Al = 1:1) and $Ni/ZnO{\cdot}Al_2O_3$ (Zn:Al = 1:2) catalysts. In addition, the introduction of palladium into Ni catalysts decreases of the $NiAl_2O_4$ spinel structure formation, which has been reported by Lakhapatri et al. [34]. This result explains the decrease of the total acidity in the case of the bimetallic catalysts compared to the $Ni/ZnO{\cdot}Al_2O_3$ (Zn:Al = 1:1) system. In addition, the introduction 2 wt% of Pd caused an increase of the total acidity compared to the 0.5%Pd–20%Ni catalyst. It was also proven that this system exhibited higher activity in the studied reaction what can be explained by a greater amount of the strong acid centers present on the catalyst surface compared to the bimetallic catalyst with a lower content of Pd.

Phase composition studies

X-ray diffraction studies were used to determine the phase composition of each catalytic system and the interaction between an active phase components and the support. Fig. 6 shows X-ray diffraction curves for nickel supported catalysts calcined in air atmosphere at 400 °C for 4 h. The XRD diffractograms recorded for Ni catalysts supported on $ZnO{\cdot}Al_2O_3$ (Zn:Al = 2:1) showed the occurrence of following crystallographic phases: NiO, ZnO and $ZnAl_2O_4$. The analysis of the XRD patterns recorded for other monometallic nickel catalysts showed only the presence of diffraction peaks attributed to the spinel $ZnAl_2O_4$ structure phase. The lack of the diffraction peaks originating from NiO indicates the formation of $NiAl_2O_4$, which took place during the preparation step of the investigated catalytic systems. It is well documented in the literature that $ZnAl_2O_4$ and $NiAl_2O_4$ spinel phases are isostructural. That is why the distinction of these phases from each other by XRD technique is rather impossible due to the fact that reflexes assigned to both structures occur in the same position of the 2θ angle [37]. Battiston et al. [38] investigated the phase composition of the $ZnAl_2O_4$ structure, which was used in photocatalysis. The XRD pattern recorded for this system shows diffraction peaks attributed to the crystallographic phase $ZnAl_2O_4$ positioned at 2θ angle: 31.2°, 36.75°, 44.7°, 49.1°, 55.6°, 59.3° and 65.3°. Yang et al. [39] studied the properties of $Ni–Ce/Al_2O_3$ catalysts used in the steam reforming of methane and other hydrocarbons. They observed that the diffractogram recorded for this catalyst

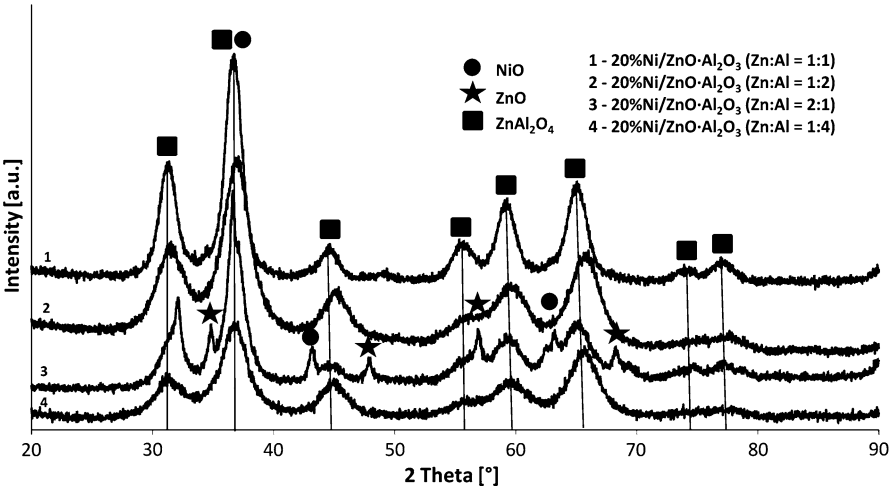

Fig. 6 XRD patterns of monometallic nickel supported catalysts calcined in an air atmosphere at 400 °C for 4 h

showed the presence of diffraction peaks attributed to the NiO phase positioned at $2\theta = 37.2°$, 43.3°, 62.9°. In our previous work [40, 41], we studied the physicochemical properties of $Cu/ZnAl_2O_4$ catalysts. We reported that during the preparation of the copper supported catalysts we confirmed the spinel $CuAl_2O_4$ structure formation. In addition, we also did not see this phase in the XRD patterns, but we confirmed the formation of it by temperature programmed reduction. We have seen the high temperature reduction stage on the TPR profile recorded for copper catalysts and the occurrence of this stage is assigned to copper aluminate structure reduction.

We also investigated the phase composition of 10%Ni catalysts supported on Al_2O_3 [29]. We did not observe the diffraction peaks originating from the spinel structure on the XRD curve, but we detected the high temperature reduction peak on the TPR profile recorded for this system, which was assigned to the $NiAl_2O_4$ reduction. Salhi et al. [42] studied $NiAl_2O_4$ and $Ni/NiAl_2O_4$ catalysts in the steam reforming of methane. They prepared catalysts via the sol–gel method and calcined these systems at 725, 800 and 900 °C. They studied the phase composition of such systems and reported that for $NiAl_2O_4$ they observed only spinel structure phase on the XRD curve. In the case of the $Ni/NiAl_2O_4$ catalysts, they detected both spinel structure and NiO phases on the diffraction curves recorded for these supported catalysts. Zhang et al. [43] studied various nickel supported catalysts and they reported that the effect of the Ni/Al ratio is very important from the reduction point of view of NiO species. They reported about three different interactions of nickel oxide with the carrier. The low temperature reduction stage is connected with unbound NiO species reduction [44, 45]. The next hydrogen consumption effect located in the temperature range 550–675 °C is assigned to the NiO in strong

interactions with the support [46]. Furthermore, the high temperature effect is attributed to the $NiAl_2O_4$ reduction located in the temperature range 800–900 °C.

Catalytic evaluation of the catalysts

The catalytic activity of monometallic 20% Ni catalysts supported on various binary oxides in OSRM was investigated in this work. The results of the catalytic activity tests performed for monometallic and bimetallic catalysts are given in Figs. 7 and 8, respectively. The catalytic tests were performed at two temperature 250 and 300 °C and the results were expressed as methanol conversion and selectivity to each product. Before of each catalytic test, the catalytic system was previously reduced at 300 °C for 1 h in a mixture of 5% H_2–95% Ar. The methanol conversion results for monometallic supported catalysts are given in Fig. 7.

Activity measurements carried out in OSRM reaction for monometallic systems showed that the highest methanol conversion at 250 °C exhibited 20% Ni/$ZnO{\cdot}Al_2O_3$ catalyst (Zn:Al = 1:4). On the other hand, at a temperature of 300 °C, the most active was 20% Ni/$ZnO{\cdot}Al_2O_3$ system (Zn:Al = 1:1). Fig. 8 presents the catalytic activity results obtained for bimetallic 0.5% Pd–20%Ni/$ZnO{\cdot}Al_2O_3$ (Zn:Al = 1:4) and 2% Pd–20% Ni/$ZnO{\cdot}Al_2O_3$ (Zn:Al = 1:4) catalysts. The activity results obtained in OSRM process for bimetallic supported catalysts showed that promotion of monometallic nickel catalyst improves the methanol conversion values at both studied temperatures of the reaction (see Fig. 8).

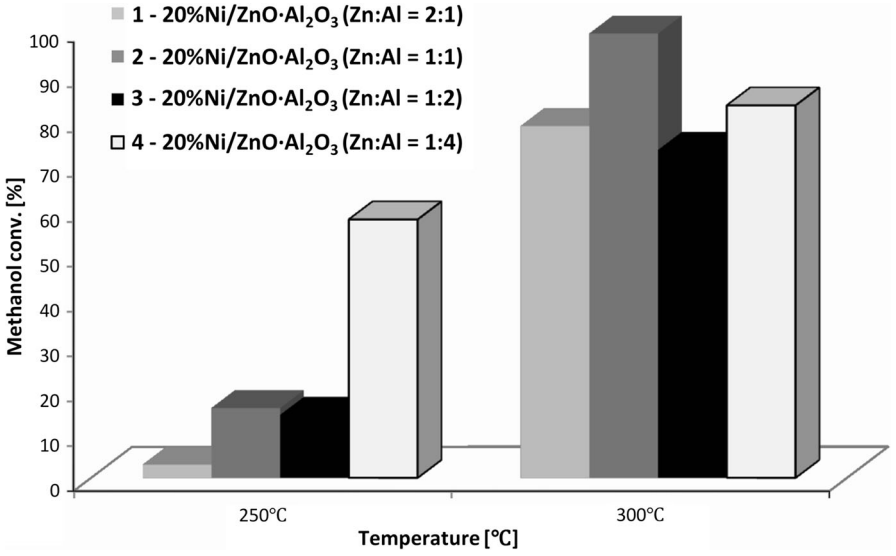

Fig. 7 The effect of support composition on the methanol conversion value in the oxy-steam reforming of methanol over monometallic nickel supported catalysts. Reaction conditions: weight of catalyst = 0.1 g, $H_2O/CH_3OH/O_2$ ratio in the feed = 1/1/0.4, temperature = 250 and 300 °C, atmospheric pressure, GHSV = 26,700 h^{-1}

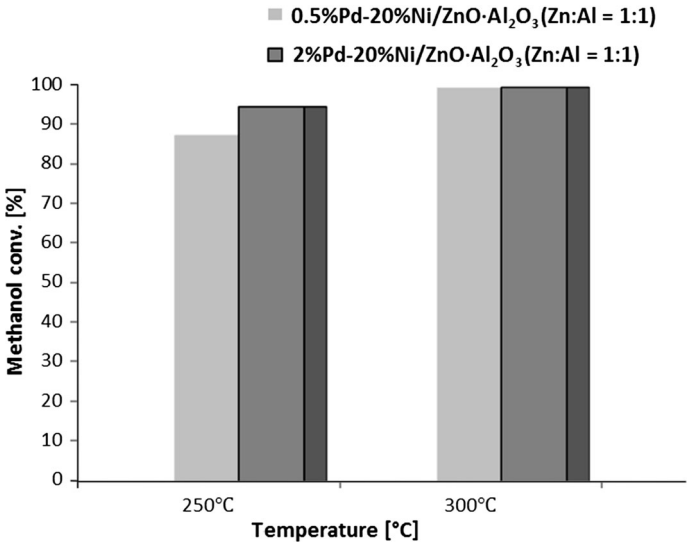

Fig. 8 The influence of the palladium on the catalytic performance of nickel catalyst in the oxy-steam reforming of methanol reaction. Reaction conditions: weight of catalyst = 0.1 g, $H_2O/CH_3OH/O_2$ ratio in the feed = 1/1/0.4, temperature = 250 and 300 °C, atmospheric pressure, GHSV = 26,700 h^{-1}

The results of the activity tests for bimetallic catalysts indicate that both systems are very active in the studied temperatures. The improvement of the catalytic activity is explained by the increase of the methanol adsorption during the oxy-steam reforming of methanol process after palladium promotion of nickel catalyst. Another important factor which influences the activity of the bimetallic catalysts in OSRM process is the facilitation of the reducibility of Ni catalysts by the addition of palladium [19]. Additionally, the bimetallic 2%Pd–20% $Ni/ZnO{\cdot}Al_2O_3$ (Zn:Al = 1:1) catalyst had a larger number of strong acid sites on its surface as compared to a catalyst with a lower content of palladium, what can explain the observed activity results.

The catalytic activity tests carried out for all systems in OSRM at 250 °C allow to present the reactivity of the catalysts by the following row: 2%Pd–20% $Ni/ZnO{\cdot}Al_2O_3$ (Zn:Al = 1:1) > 0.5–20% $Ni/ZnO{\cdot}Al_2O_3$ (Zn:Al = 1:1) > 20% $Ni/ZnO{\cdot}Al_2O_3$ (Zn:Al = 1:4) > 20% $Ni/ZnO{\cdot}Al_2O_3$ (Zn:Al = 1:1) ≈ 20% $Ni/ZnO{\cdot}Al_2O_3$ (Zn:Al = 1:2) > 20% $Ni/ZnO{\cdot}Al_2O_3$ (Zn:Al = 2:1). The series of the catalytic activities for all catalysts at 300 °C can be described in the following order: 2%Pd–20% $Ni/ZnO{\cdot}Al_2O_3$ (Zn:Al = 1:1) ≈ 0.5–20% $Ni/ZnO{\cdot}Al_2O_3$ (Zn:Al = 1:1) ≈ 20% $Ni/ZnO{\cdot}Al_2O_3$ (Zn:Al = 1:1) > 20% $Ni/ZnO{\cdot}Al_2O_3$ (Zn:Al = 1:4) > 20% $Ni/ZnO{\cdot}Al_2O_3$ (Zn:Al = 2:1) > 20% $Ni/ZnO{\cdot}Al_2O_3$ (Zn:Al = 1:2).

The methanol conversion values showed that the increase of the OSRM reaction temperature from 250 to 300 °C has influence on the catalytic activity. All systems showed the highest methanol conversion at higher temperature. It is also worth emphasizing that the most active system at both temperatures was 2% Pd–20% Ni/

$ZnO{\cdot}Al_2O_3$ (Zn:Al = 1:1) system. The methanol conversion values of bimetallic catalysts confirmed also that catalyst which exhibited higher total acidity was more active catalyst and had the higher amount of a strong acid sites on the catalyst surface compared to the 0.5% Pd–20% $Ni/ZnO{\cdot}Al_2O_3$ (Zn:Al = 1:1) catalyst. These results indicate that the acid centers play crucial role during the oxy-steam reforming of methanol reaction. It was also proven that among of all monometallic catalyst systems the highest active in the investigated process at 300 °C was the system which was characterized by the highest total acidity. This result confirmed that this system showed the most stabilizing effect of the intermediate formed on the catalyst surface during the reaction and agree well with the work [7]. Hereijgers et al. [47] also reported that the acidic centers which are present on the catalysts surface play important role during the reaction and explain the activity of the studied system in the oxidation of methanol to hydrogen. The selectivity results towards hydrogen, carbon monoxide, carbon dioxide and dimethyl ether formation at both temperatures 250 and 300 °C are also evaluated in this work and the results are presented in Table 3. The selectivity results obtained for Ni supported catalysts showed that the increase of the Al content in the catalytic system causes the decrease of the selectivity towards hydrogen production. The highest selectivity to hydrogen formation among all nickel supported catalysts was exhibited by the 20% $Ni/ZnO{\cdot}Al_2O_3$ (Zn:Al = 1:1) system, while the lowest selectivity to hydrogen was found for the 20% $Ni/ZnO{\cdot}Al_2O_3$ (Zn:Al = 1:4) catalyst. The promotion of a nickel catalysts by palladium improves the selectivity to hydrogen formation at both temperatures of the reaction. An important result is the lack of carbon monoxide formation as a by-product of the reaction carried out over 20% $Ni/ZnO{\cdot}Al_2O_3$ (Zn:Al = 1:1) and 20% $Ni/ZnO{\cdot}Al_2O_3$ (Zn:Al = 2:1) catalysts. This is a very important result from the application point of view. CO is very strong poison of the electrodes used in fuel cells technology. It is also worth emphasizing that the limit of detection of CO compound by TCD detector is in the range of 5–50 ng. Based on the above information, we cannot rule out the formation of carbon monoxide in an amount below the detection of the TCD detector [9, 48]. The highest activity of monometallic Ni catalyst in the OSRM reaction at 300 °C was 20% $Ni/ZnO{\cdot}Al_2O_3$ (Zn:Al = 1:1) system. In the case of this system, only CO_2 and H_2 products were observed in the final product. In addition, at a lower temperature, this catalyst showed the same product formation. The addition of palladium to the most active monometallic nickel supported catalyst 20% $Ni/ZnO{\cdot}Al_2O_3$ (Zn:Al = 1:1) improves the selectivity towards hydrogen formation at both studied temperatures. It is also worth mentioning that palladium promotion improves the selectivity towards CO formation during the reaction. Summarizing the activity results, it can be concluded that the observed results can be related with the total acidity, reducibility and the composition of the catalyst. The obtained results also confirm the dependence of the catalytic activity on the number of the strong acid sites present on the catalyst surface. The monometallic catalytic system which had the highest quantity of the strong acid sites exhibited the highest activity in OSRM reaction. In addition, the most active bimetallic catalysts were the easiest reduced catalysts. These findings also correlate well with the results obtained by Pérez-Hernández et al. [12]. The authors of the work [12] reported that the activities of the

Table 3 Activity and selectivity results in the oxy-steam reforming of methanol over monometallic nickel and bimetallic catalysts supported on binary oxides

Catalyst	CH_3OH conversion (%)		H_2 selectivity (%)		CO selectivity (%)		CO_2 selectivity (%)		DME selectivity (%)	
	250 °C	300 °C	250 °C	300 °C	250 °C	300 °C	250 °C	300 °C	250 °C	300 °C
20% Ni/ZnO·Al_2O_3 (Zn:Al = 2:1)	3	78	17	76	0	0	83	24	0	0
20% Ni/ZnO·Al_2O_3 (Zn:Al = 1:1)	16	99	66	76	0	0	34	24	0	0
20% Ni/ZnO·Al_2O_3 (Zn:Al = 1:2)	14	73	60	40	0	10	30	24	10	26
20% Ni/ZnO·Al_2O_3 (Zn:Al = 1:4)	58	83	43	65	0	0	0	21	57	14
0.5%Pd–20% Ni/ZnO·Al_2O_3 (Zn:Al = 1:1)	87	99	72	73	10	10	18	17	0	0
2%Pd–20% Ni/ZnO·Al_2O_3 (Zn:Al = 1:1)	94	99	73	72	10	8	17	20	0	0

Reaction condition: weight of catalyst = 0.2 g, $H_2O/CH_3OH/O_2$ ratio in the feed = 1/1/0.4, temperature = 250 and 300 °C, atmospheric pressure, GHSV = 26,700 h^{-1}

nickel supported catalysts were related with their specific surface area, the composition of the support, their reducibility as well as with the quantity of metallic centers present on the catalyst surface.

Conclusions

The production of hydrogen via OSRM reaction was effectively carried out on the investigated mono- and bimetallic nickel catalysts supported on various $ZnO{\cdot}Al_2O_3$ systems. The reactivity results obtained for the investigated catalysts depend strongly on the support composition. In addition, the promotion effect of palladium on the catalytic activity and selectivity towards hydrogen production of nickel supported catalysts in OSRM was proven. We have demonstrated that the activity and selectivity in the investigated reaction depends on the acidity (especially strong acid centers) and reducibility of the studied systems. It was also confirmed that palladium addition facilitates the reducibility of the nickel supported catalysts. The results obtained within the work indicate that nickel and palladium–nickel supported catalysts may be potentially applied in fuel cells technology. The prepared catalysts can potentially be used as an anode material for a solid oxide fuel cell (SOFC) technology.

Acknowledgements This work was funded by Polish Ministry of Science and Higher Education within the "Iuventus Plus" Programme (2015–2017) (Project No. 0305/IP2/2015/73).

Compliance with ethical standards

Conflict of interest The authors declare that there is no conflict of interest regarding the publication of this paper.

References

1. Nikolaidis P, Poullikkas A (2017) A comparative overview of hydrogen production processes. Renew Sustain Energy Rev 67:597–611
2. Sharma PK, Saxena N, Roy PK, Bhatt A (2016) Hydrogen generation from ethanol by steam reforming using a Rh catalyst supported over low acidic Al_2O_3. React Kinet Mech Catal 117:655–674
3. Mierczynski P, Vasilev K, Mierczynska A, Maniukiewicz W, Maniecki TP (2014) Highly selective Pd–Cu/$ZnAl_2O_4$ catalyst for hydrogen production. Appl Catal A 479:26–34
4. Mierczynski P, Vasilev K, Mierczynska A, Maniukiewicz W, Maniecki TP (2013) The effect of $ZnAl_2O_4$ on the performance of Cu/$Zn_xAl_yO_{x+1.5y}$ supported catalysts in steam reforming of methanol. Top Catal 56:1015–1025

5. Turco M, Bagnasco G, Cammarano C, Senese P, Costantino U, Sisani M (2007) Cu/ZnO/Al_2O_3 catalysts for oxidative steam reforming of methanol: the role of Cu and the dispersing oxide matrix. Appl Catal B 77:46–57
6. Chang FW, Ou TC, Roselin LS, Chen WS, Lai SC, Wu HM (2009) Production of hydrogen by partial oxidation of methanol over bimetallic Au–Cu/TiO_2–Fe_2O_3 catalysts. J Mol Catal A 313:55–64
7. Mierczynski P, Vasilev K, Mierczynska A, Ciesielski R, Maniukiewicz W, Rogowski J, Szynkowska IM, Trifonov AY, Gromov D, Dubkov SV, Maniecki TP (2016) The effect of gold on modern bimetallic Au–Cu/MWCNT catalysts for oxy-steam reforming of methanol. Catal Sci Technol 6:4168–4183
8. Mierczynski P, Ciesielski R, Kedziora A, Nowosielska M, Kubicki J, Maniukiewicz W, Czylkowska A, Maniecki TP (2016) Monometallic copper catalysts supported on multi-walled carbon nanotubes for the oxy-steam reforming of methanol. React Kinet Mech Catal 117:675–691
9. Mierczynski P, Vasilev K, Mierczynska A, Maniukiewicz W, Szynkowska MI, Maniecki TP (2016) Bimetallic Au–Cu, Au–Ni catalysts supported on MWCNTs for oxy-steam reforming of methanol. Appl Catal B 185:281–294
10. López P, Mondragón-Galicia G, Espinosa-Pesqueira ME, Mendoza-Anaya D, Fernández ME, Gómez-Cortés A, Bonifacio J, Martínez-Barrera G, Pérez-Hernández R (2012) Hydrogen production from oxidative steam reforming of methanol: effect of the Cu and Ni impregnation on ZrO_2 and their molecular simulation studies. Int J Hydrog Energy 37:9018–9027
11. Pérez-Hernández R, Mondragón Galicia G, Mendoza Anaya D, Palacios J, Angeles-Chavez C, Arenas-Alatorre J (2008) Synthesis and characterization of bimetallic Cu–Ni/ZrO_2 nanocatalysts: H_2 production by oxidative steam reforming of methanol. Int J Hydrog Energy 33:4569–4576
12. Pérez-Hernández R, Gutiérrez-Martínez A, Palacios J, Vega-Hernández M, Rodríguez-Lugo V (2011) Hydrogen production by oxidative steam reforming of methanol over Ni/CeO_2–ZrO_2 catalysts. Int J Hydrog Energy 36:6601–6608
13. Pérez-Hernández R, Gutiérrez-Martínez A, Espinosa-Pesqueira ME, Estanislao ML, Palacios J (2015) Effect of the bimetallic Ni/Cu loading on the ZrO_2 support for H_2 production in the autothermal steam reforming of methanol. Catal Today 250:166–172
14. Chang CC, Chang CT, Chiang SJ, Liaw BJ, Chen YZ (2010) Oxidative steam reforming of methanol over CuO/ZnO/CeO_2/ZrO_2/Al_2O_3 catalysts. Int J Hydrog Energy 35:7675–7683
15. Turco M, Bagnasco G, Costantino U, Marmottini F, Montanari T, Ramis G, Busca G (2004) Production of hydrogen from oxidative steam reforming of methanol: I. Preparation and characterization of Cu/ZnO/Al_2O_3 catalysts from a hydrotalcite-like LDH precursor. J Catal 228:43–55
16. Liu S, Takahashi K, Eguchi H, Uematsu K (2007) Hydrogen production by oxidative methanol reforming on Pd/ZnO: catalyst preparation and supporting materials. Catal Today 129:287–292
17. Liu S, Takahashi K, Fuchigami K, Uematsu K (2006) Hydrogen production by oxidative methanol reforming on Pd/ZnO: catalyst deactivation. Appl Catal A 299:58–65
18. Chang CC, Hsu CC, Chang CT, Chen YP, Liaw BJ, Chen YZ (2012) Effect of noble metal on oxidative steam reforming of methanol over CuO/ZnO/Al_2O_3 catalysts. Int J Hydrog Energy 37:11176–11184
19. Mierczynski P (2016) Comparative studies of bimetallic Ru–Cu, Rh–Cu, Ag–Cu, Ir–Cu catalysts supported on ZnO–Al_2O_3, ZrO_2–Al_2O_3 systems. Catal Lett 146:1825–1837
20. Pairojpiriyakul T, Croiset E, Kiatkittipong K, Kiatkittipong W, Arpornwichanop A, Assabumrungrat S (2014) Catalytic reforming of glycerol in supercritical water with nickel-based catalysts. Int J Hydrog Energy 39:14739–14750
21. Zhao X, LÜ Y, Liao W, Jin M, Suo Z (2015) Hydrogen production from steam reforming of ethylene glycol over supported nickel catalysts. J Fuel Chem Technol 43:581–588
22. Kobayashi Y, Horiguchi J, Kobayashi S, Yamazaki Y, Omata K, Nagao D, Konno M, Yamada M (2011) Effect of NiO content in mesoporous NiO–Al_2O_3 catalysts for high pressure partial oxidation of methane to syngas. Appl Catal A 395:129–137
23. Li G, Hu L, Hill JM (2006) Comparison of reducibility and stability of alumina-supported Ni catalysts prepared by impregnation and co-precipitation. Appl Catal A 301:16–24
24. Kim P, Kim Y, Kim H, Song IK, Yi J (2004) Synthesis and characterization of mesoporous alumina with nickel incorporated for use in the partial oxidation of methane into synthesis gas. Appl Catal A 272:157–166
25. Ding C, Liu W, Wang J, Liu P, Zhang K, Gao X, Ding G, Liu S, Han Y, Ma X (2015) One step synthesis of mesoporous NiO–Al_2O_3 catalyst for partial oxidation of methane to syngas: the role of calcination temperature. Fuel 162:148–154

26. Richardson JT, Lei M, Turk B, Forster K, Twigg MV (1994) Reduction of model steam reforming catalysts: NiO/α-Al2O3. Appl Catal A 110:217–237
27. Nieva MA, Villaverde MM, Monzón A, Garetto TF, Marchi AJ (2014) Steam-methane reforming at low temperature on nickel-based catalysts. Chem Eng J 235:158–166
28. Maniecki TP, Bawolak K, Mierczynski P, Jozwiak W (2009) Development of stable and highly active bimetallic Ni–Au catalysts supported on binary oxides $CrAl_{(3)}O_{(6)}$ for POM reaction. Catal Lett 128:401–404
29. Maniecki TP, Stadnichenko A, Maniukiewicz W, Bawolak K, Mierczynski P, Boronin A, Jozwiak W (2010) An active phase transformation on surface of Ni–Au/Al_2O_3 catalyst during partial oxidation of methane to synthesis gas. Kinet Catal 51:573–578
30. Maniecki TP, Mierczynski P, Maniukiewicz W, Bawolak K, Gebauer D, Jozwiak W (2009) Bimetallic Au–Cu, Ag–Cu/$CrAl_3O_6$ catalysts for methanol synthesis. Catal Lett 130:481–488
31. Mierczynski P, Ciesielski R, Kedziora A, Shtyka O, Maniecki TP (2017) Methanol synthesis using copper catalysts supported on $CeO_2-Al_2O_3$ mixed oxide. Fibre Chem 48:271–275
32. Xu J, Su X, Liu X, Pan X, Pei G, Huang Y, Wang X, Zhang T, Geng H (2016) Methanol synthesis from CO_2 and H_2 over Pd/ZnO/Al_2O_3: catalyst structure dependence of methanol selectivity. Appl Catal A 514:51–59
33. Cárdenas-Lizana F, Gómez-Quero S, Amorim C, Keane MA (2014) Gas phase hydrogenation of p-chloronitrobenzene over Pd–Ni/Al_2O_3. Appl Catal A 473:41–50
34. Lakhapatri SL, Abraham MA (2011) Analysis of catalyst deactivation during steam reforming of jet fuel on Ni-(PdRh)/γ-Al2O3 catalyst. Appl Catal A 405:149–159
35. Mierczynski P, Chalupka KA, Maniukiewicz W, Kubicki J, Szynkowska MI, Maniecki TP (2015) $SrAl_2O_4$ spinel phase as active phase of transesterification of rapeseed oil. Appl Catal B 164:176–183
36. Mierczynski P, Ciesielski R, Kedziora A, Maniukiewicz W, Shtyka O, Kubicki J, Albinska J, Maniecki TP (2015) Biodiesel production on MgO, CaO, SrO and BaO oxides supported on (SrO)(Al_2O_3) mixed oxide. Catal Lett 145:1196–1205
37. Barroso MN, Gomez MF, Gamboa JA, Arrúa LA, Abello MC (2006) Preparation and characterization of CuZnAl catalysts by citrate gel process. J Phys Chem Solids 67:1583–1589
38. Battiston S, Rigo C, Severo EC, Mazutti MA, Kuhn RC, Gündel A, Foletto EL (2014) Synthesis of zinc aluminate ($ZnAl_2O_4$) spinel and its application as photocatalyst. Mater Res 17:734–738
39. Yang X, Da J, Yu H, Wang H (2016) Characterization and performance evaluation of Ni-based catalysts with Ce promoter for methane and hydrocarbons steam reforming process. Fuel 179:353–361
40. Mierczynski P, Maniecki TP, Chalupka K, Maniukiewicz W, Jozwiak WK (2011) Cu/$Zn_xAl_yO_z$ supported catalysts (ZnO:Al_2O_3 = 1, 2, 4) for methanol synthesis. Catal Today 176:21–27
41. Mierczynski P, Maniukiewicz W, Maniecki T (2013) Comparative studies of Pd, Ru, Ni, Cu/$ZnAl_2O_4$ catalysts for the water gas shift reaction. Cent Eur J Chem 11:912–919
42. Salhi N, Boulahouache A, Petit C, Kiennemann A, Rabia C (2011) Steam reforming of methane to syngas over $NiAl_2O_4$ spinel catalysts. Int J Hydrog Energy 36:11433–11439
43. Zhang L, Lin J, Chen Y (1992) Characterization of dispersion and surface states of NiO/[gamma]-alumina and NiO/La_2O_3-[gamma]-alumina catalysts. J Chem Soc Faraday Trans 88:497–502
44. O'Connor AM, Schuurman Y, Ross JRH, Mirodatos C (2006) Transient studies of carbon dioxide reforming of methane over Pt/ZrO_2 and Pt/Al_2O_3. Catal Today 115:191–198
45. Teixeira ACSC, Giudici R (1999) Deactivation of steam reforming catalysts by sintering: experiments and simulation. Chem Eng Sci 54:3609–3618
46. Al-Ubaid A, Wolf EE (1988) Steam reforming of methane on reduced non-stoichiometric nickel aluminate catalysts. Appl Catal 40:73–85
47. Hereijgers BPC, Weckhuysen BM (2009) Selective oxidation of methanol to hydrogen over gold catalysts promoted by alkaline-earth-metal and lanthanum oxides. ChemSusChem 2:743–748
48. Cazes Jack (2006) Encyclopedia of chromatography, 2nd edn. Taylor & Francis, Bocaraton